Lawrence Berkeley National Laboratory

Title

Unique Diacidic Fragments Inhibit the OXA-48 Carbapenemase and Enhance the Killing of Escherichia coli Producing OXA-48

Permalink

https://escholarship.org/uc/item/7rh7j0f2

Journal

ACS Infectious Diseases, 7(12)

ISSN

2373-8227

Authors

Taylor, Doris Mia
Anglin, Justin
Hu, Liya
et al.

Publication Date

2021-12-10

DOI

10.1021/acsinfecdis.1c00501

Copyright Information

Peer reviewed

Unique Diacidic Fragments Inhibit the OXA-48 Carbapenemase and Enhance the Killing of *E. coli* Producing OXA-48

Doris Mia Taylor[1], **Justin Anglin**[2,3], **Liya Hu**[1], **Lingfei Wang**[4], **Banumathi Sankaran**[5], **Jin Wang**[4], **Martin M. Matzuk**[2,3,4], **B.V. Venkataram Prasad**[1], **Timothy Palzkill**[1,4,*]

[1]Verna and Marrs McLean Department of Biochemistry and Molecular Biology, Baylor College of Medicine, Houston, TX, 77030, USA

[2]Center for Drug Discovery, Baylor College of Medicine, Houston, TX, 77030, USA

[3]Department of Pathology & Immunology, Baylor College of Medicine, Houston, TX, 77030, USA

[4]Department of Pharmacology and Chemical Biology, Baylor College of Medicine, Houston, TX, 77030, USA

[5]Molecular Biophysics and Integrated Bioimaging, Berkeley Center for Structural Biology, Advanced Light Source, Lawrence Berkeley National Laboratory, CA, 94720, USA

Abstract

Despite advances in β-lactamase inhibitor development, limited options exist for the class D carbapenemase known as OXA-48. OXA-48 is one of the most prevalent carbapenemases in carbapenem-resistant *Enterobacteriaceae* infections and is not susceptible to most available β-lactamase inhibitors. Here, we screened various low molecular weight compounds (fragments) against OXA-48 to identify functional scaffolds for inhibitor development. Several biphenyl-, naphthalene-, fluorene-, anthraquinone-, and azobenzene-based compounds were found to inhibit OXA-48 with low micromolar potency despite their small size. Co-crystal structures of OXA-48 with several of these compounds revealed key interactions with the carboxylate binding pocket, Arg214, and various hydrophobic residues of β-lactamase that can be exploited in future inhibitor development. A number of the low micromolar potency inhibitors, across different scaffolds, synergize with ampicillin to kill *E. coli* expressing OXA-48, albeit at high concentrations of the respective inhibitors. Additionally, several compounds demonstrated micromolar potency towards the OXA-24 and OXA-58 class D carbapenemases that are prevalent in *Acinetobacter baumannii*. This work provides foundational information on a variety of chemical scaffolds that can guide the design of effective OXA-48 inhibitors that maintain efficacy as well as potency towards other major class D carbapenemases.

Graphical Abstract
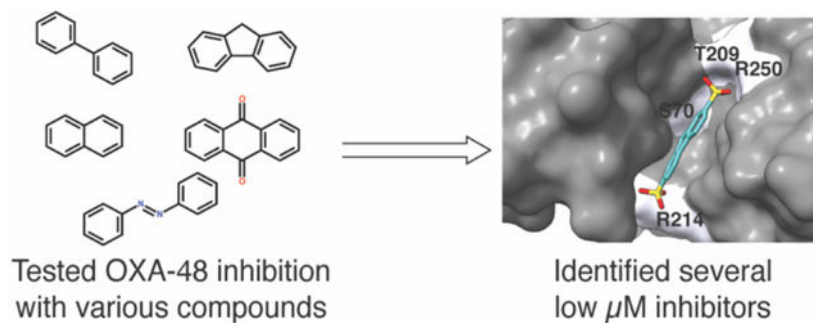
The graphic shows the variety of scaffolds of the compounds tested against the OXA-48 carbapenemase and a co-crystal structure of OXA-48 with a fluorene-based inhibitor. The work reveals how various monoacidic and diacidic fragment-based compounds bind and inhibit OXA-48 as well as their efficacy against *E. coli in vitro* despite their small size.

Keywords

antibiotic resistance; β -lactam; β -lactamase; inhibitor; carbapenemase; OXA-48; Class D carbapenemase; drug discovery; fragment inhibitors

Carbapenem antibiotics of the larger β-lactam antibiotic family are among the few last resort options for multidrug-resistant infections.[1] Unfortunately, carbapenem utility is challenged by the increasing prevalence and dissemination of carbapenem-inactivating β-lactamases (carbapenemases) across problematic Gram-negative bacteria.[2–4] β-lactamase inhibitors can be developed to block β-lactamase activity and paired with the antibiotics in combination treatments to maintain the effectiveness of these drugs against β-lactamase-producing bacteria.[5] However, the proliferation of broad-spectrum carbapenemases that are not susceptible to current inhibitors is a cause for concern.[1] β-lactamase enzymes are grouped by sequence homology into classes A – D, where the class A, C, and D enzymes are serine hydrolases, and class B are zinc metalloenzymes.[6] The class A, C and D carbapenemases confer resistance to carbapenems and other clinically relevant β-lactams in pathogenic bacteria worldwide.[2] Despite advances in the development of serine β-lactamase inhibitors, many of them are less potent against class D carbapenemases.[7] The most prevalent class D carbapenemase, Oxacillinase-48 (OXA-48), confers carbapenem resistance in several multidrug-resistant, Gram-negative pathogens across the globe, most commonly in *Klebsiella pneumoniae*.[3,4]

Class D β-lactamases use an active site serine (Ser70) and a carbamylated lysine (KCX73) for β-lactam hydrolysis (OXA-48 numbering).[8–10] Ser70 attacks the β-lactam ring and forms a covalent, acyl-enzyme complex, that is subsequently attacked by an enzyme-activated water molecule to hydrolyze the antibiotic. The KCX73 residue is post-translationally modified by CO_2 and the resulting carboxylate group functions as a general base, activating both Ser70 for acylation and the active site water for deacylation of the covalent intermediate. The active site of class D enzymes also contains a number of

conserved hydrophobic residues including Trp105, Val120, Trp157, and Ile/Leu158 that lower the pKa of the catalytic lysine (near neutral pH) to promote its carboxylation for efficient catalysis.[8,9,11,12] Class D enzymes share motifs with other serine β-lactamases such as: (i) an additional serine residue that serves as a proton shuttle (Ser118) to the leaving group nitrogen of the β-lactam amide, (ii) an oxyanion hole to stabilize anionic intermediates formed during catalysis (Ser70 and Trp/Tyr211), and (iii) a carboxylate binding pocket to facilitate substrate binding and stabilize reaction intermediates (Ser118, Ser/Thr209, and Arg250).[8,13–15] Despite similarities with other serine β-lactamases, inhibition of class D β-lactamases such as OXA-48 has been more elusive and understudied.

To identify unique compounds that can inform the design of novel OXA-48 inhibitors, we screened low molecular weight compounds (fragments) containing carboxylate or sulfonic acid groups for potency against OXA-48. Fragment-based drug discovery (FBDD) can identify ligand efficient binders that can subsequently be developed into compounds with enhanced potency.[16,17] Moreover, this approach allows chemical sampling and binding site probing to identify novel scaffolds and useful protein-ligand interactions. FBDD has proven useful for studying β-lactamase inhibition and developing non-covalent OXA-48 inhibitors with micromolar potency.[18–21] We identified biphenyl-, naphthalene, and fluorene-based OXA-48 inhibitors with low micromolar potency despite their small size. Crystal structures for several compounds in complex with OXA-48 showed key enzyme residues involved in the binding that can be exploited in future inhibitor designs. Moreover, these compounds showed potency against other class D carbapenemases including OXA-58, and to a lesser extent OXA-24. These OXA-carbapenemases are an important source of resistance in *Acinetobacter baumannii* and thus are relevant inhibitor targets.[3,22] Also, a unique azobenzene-based compound showed similar low micromolar potency against OXA-48 and both OXA-24 and OXA-58, despite sequence and structural differences between the enzymes. Most promisingly, at high concentrations, all of the low micromolar potency OXA-48 inhibitors identified (K_i < 10 μM) showed synergy with ampicillin *in vitro* against *E. coli* expressing OXA-48. The biochemical and structural insights gained here can help in the design of novel OXA-48 inhibitors with increased potency and that accumulate through the Gram-negative outer membrane as well as show efficacy against other class D carbapenemases.

Results and Discussion

Low MW compounds with unique scaffolds inhibit OXA-48

Based on our previous findings from DNA-encoded chemical libraries as well as published studies on fragment-based inhibitors that carboxylate or sulfonic acid groups make key interactions with the active site of OXA-48[15,18,19], we selected and screened a variety of low molecular weight compounds for inhibition of purified OXA-48 enzyme to identity novel scaffolds that can inform inhibitor design. Aromatic rings present in previously reported OXA-48 inhibitors were shown to make hydrophobic and pi-stacking interactions in the active site[18,19], while acid groups interacted with the carboxylate binding pocket. Therefore, we selected compounds that contained at least one aromatic ring and up to two acid groups (-COOH or SO$_3$) to increase the likelihood of identifying inhibitors. Given that biphenyl-

and naphthalene-based fragments inhibit OXA-48 with micromolar potency[18,19], we tested unique compounds in these two classes. For comparison, we also tested novel fluorene-, anthraquinone-, and azobenzene-based compounds with aromatic ring systems to determine the potential of these scaffolds for inhibition of OXA-48. While these unique scaffolds have not been explicitly tested on β-lactamases previously, dichloro-fluorene derivatives and azobenzenes have been reported to show antibacterial activity[23,24] and anthraquinone dyes have been found to bind early class D β-lactamases.[25] The selected compounds broadly followed the 'Rule of 3' for fragments with a molecular weight < 300 Da, hydrogen bond donors 3, hydrogen bond acceptors 3, and a cLogP 3.[26] The potency of OXA-48 inhibition for each compound was determined using inhibition assays with the chromogenic β-lactam nitrocefin as the reporter substrate. Additionally, the ligand efficiency (LE) was calculated for each compound based on the inhibition constant (Methods).

Several of the compounds inhibited OXA-48 with low micromolar potency and LE values (Table 1). Although LE alone is not a suitable parameter for ranking compounds[27], typically compounds with an LE 0.3 are the most promising for further development since a theoretical 500-Da (~38 heavy atoms) drug candidate with 10 nM potency would have an LE of 0.29.[28] The most ligand efficient compounds (LE 0.40) were biphenyl- and naphthalene-based, with the most ligand efficient being compound **2.3** (LE = 0.44). Compound **2.3** has a similar configuration as some 3-aryl-substituted benzoic acids tested by Akhter et al.[19] Although those compounds appear to be lower in potency and ligand efficiency than compound **2.3**, the meta-substitution is a useful property to consider for OXA-48 inhibitor development. The utility of a meta-substitution for biphenyl inhibitors is also shown with compound **2.3** being more potent (~10-fold) and more ligand efficient (+ 0.07), than its isomer (compound **2.1**) arranged in a para-substituted. For the naphthalenes, compound **3.1** was the most potent and ligand efficient (K_i = 5.1 μM; LE = 0.40). Although weaker inhibitors, the other naphthalenes underscore how the addition of a polar group can be beneficial for the potency. Compounds **3.2** – **3.5** can be seen as two pairings (**3.2** and **3.3** vs. **3.4** and **3.5**), in which the compounds are nearly identical except the latter compound of each pair has an additional polar group that improves potency ~ 3 – 4-fold (Table 1).

Compound **4.3**, the only diacidic fluorene-based compound tested, had a low micromolar K_i and an LE of 0.38, highlighting the potential of fluorene-based compounds for OXA-48 inhibition. The monoacidic anthraquinones, compounds **5.1** and **5.2**, are relatively weak inhibitors of OXA-48, with K_i values above 50 μM (Table 1). Based on previously published inhibitors[18,19], compounds with two acid groups can allow additional hydrogen bonding, so it is not surprising that the monoacids tested (compounds **4.1**, **4.2**, **5.1**, and **5.2**) show low potency. Nevertheless, the monoacidic anthraquinones (**5.1**, **5.2**) are significantly more potent than the monoacidic fluorenes (**4.1**, **4.2**), highlighting the potential of this unique scaffold. While anthraquinones have not been widely studied as β-lactamase inhibitors, a study showed anthraquinone dyes meant to bind nucleotide-binding enzymes could inhibit an early class D β-lactamase, OXA-2, with low micromolar potency.[25] A single azobenzene, compound **6.1** was also tested and showed low micromolar potency although, on account of its size, it is not as ligand efficient as the other disulfonates (compounds **2.2**, **3.1**, and **4.3**). The activity of compound **6.1** suggests azobenzene-based compounds may serve as unique

inhibitors for OXA-48, especially given their ability to alternate between cis- and trans-configurations with UV light exposure.[29,30]

Compounds 2.2, 2.3, 3.1, 3.3, and 4.3 form hydrogen bonds, pi-stacking and hydrophobic interactions in the OXA-48 active site

The structures of the OXA-48 enzyme in complex with compounds **2.2**, **2.3**, **3.1**, **3.3**, and **4.3** were determined by X-ray crystallography (Table 2). The structures determined in the $P6_5$ space group (compounds **2.3** and **4.3**) contained four OXA-48 molecules in the asymmetric unit, while the remaining structures were determined in the $P6_522$ space group and had two OXA-48 molecules in the asymmetric unit (Table 2). For all structures, each OXA-48 molecule was bound to a molecule of the respective ligand, and all ligand occupancies were >80%. Additional information on the ligand fits for the various co-crystal structures is provided in the Supporting Information (Table S2).

All of the compounds that co-crystallized with OXA-48 were found to bind in the active site (Fig. 1). For each compound, one of the acid groups binds the carboxylate binding pocket (Ser118, Thr209, and Arg250) forming hydrogen bonds with these residues and an ionic bond with Arg250. The other acid of compounds **2.2**, **2.3**, **3.1**, and **4.3** forms hydrogen bonds with Arg214 at the base of the active site. Compound **3.3** distinctively does not interact with Arg214. While one of its sulfonic acid hydrogen bonds with Ser118, Thr209, and Arg250, the other protrudes from the active site, positioning the compound in a unique orientation compared to the other compounds. In addition to the hydrogen bonds, the compounds also made different hydrophobic interactions with various active site residues and pi-stacking interactions depending on their positioning in the active site. Compounds **2.2**, **3.3**, and **4.3** bind at angles that allow additional hydrophobic interactions with Ile102 and Trp105 in the active site. Compounds **2.3** and **3.1** make few hydrophobic interactions with Ile102, Val120 and Trp105 because of rotation of the ring system away from the hydrophobic residues. The positioning of these compounds also affected pi-stacking interactions. For example, compound **2.2** forms a π-π interaction with Trp105 whereas **3.3** forms such a bond with Tyr 211.

Despite their small size, the compounds make a variety of interactions with active site residues, consistent with their low micromolar potency. For each structure, little variation was seen in the orientation of a given ligand across the unique OXA-48 molecule chains in the asymmetric unit. Interestingly, the position of rotatable phenyl groups in compounds **2.2** and **2.3** as well as the acids of most compounds were maintained across the chains in the asymmetric unit in each structure. The sulfonic acid of compound **3.1** that interacts with Arg214 was an exception and was rotated in different positions for the two OXA-48 molecules in the asymmetric unit, although the acid interaction with the carboxylate binding pocket was the same in both OXA-48 chains. The conservation of orientations across chains in the asymmetric unit suggests that the compounds make specific, favorable interactions with OXA-48 residues and adopt a preferred pose despite their limited size and complexity.

Several compounds synergize with ampicillin to kill E. coli expressing OXA-48

Since effective β-lactamase inhibitors synergize with β-lactam antibiotics to promote bacterial death, we used minimum inhibitory concentration (MIC) assays to test whether the compounds that showed low micromolar potency of inhibition of OXA-48 would be effective against bacteria expressing OXA-48 (*E. coli*$_{OXA-48}$). The compounds were tested for the ability to reduce the MIC of ampicillin (AMP MIC), a β-lactam antibiotic readily hydrolyzed by OXA-48.[31] Since the compounds have low micromolar potency, we used an antibiotic with a high MIC in the presence of OXA-48 and a low MIC in its absence as this provides a large window of antibiotic concentrations to visualize changes in MIC due to the presence of an OXA-48 inhibitor. Since OXA-48 hydrolyzes ampicillin more efficiently than carbapenems,[31] we used ampicillin for these assays.

All the inhibitors tested were able to significantly reduce the AMP MIC by up to 256 μg/mL of the respective inhibitor (4-fold reduction from inhibitor-less control) (Table 3). At 256 μg/mL, compounds **2.2**, **2.3**, **3.1**, and **4.3** showed a 16-fold reduction in AMP MIC compared to their respective inhibitor-less control, while the remaining inhibitors showed a 4-fold reduction. The clinical breakpoint of ampicillin denotes that *E. coli* strains with MIC values 32 μg/mL are ampicillin resistant.[32] Although none of the inhibitors reduced the AMP MIC below the resistant breakpoint, their synergistic properties suggest they permeate the outer membrane of *E. coli* to reach and inhibit OXA-48 expressed in the periplasm of the cells. Given the barrier that the outer membrane permeation poses for the development of new antibacterial agents[33], the *in vitro* activity of these fragment-sized compounds suggests that, although currently not sufficiently potent to lower the MIC below the breakpoint, derivatives may be developed with enhanced activity.[15]

Several of the OXA-48 inhibitors also inhibit other major class D carbapenemases

An ideal inhibitor would inhibit a broad range of β-lactamases, and, particularly, other class D carbapenemases. Therefore, we also tested the compounds for inhibition of other class D carbapenemases *in vitro* to determine if any scaffolds are effective against these enzymes. A number of compounds showed good inhibitory activity towards OXA-24 and OXA-58 (Table 4), which are important class D carbapenemases found predominantly in carbapenem-resistant *Acinetobacter baumannii*.[34,35] Despite being from the same class, OXA-24 and OXA-58 each share only ~30% sequence identity with OXA-48 and ~53% identity with each other. Moreover, these enzymes differ from OXA-48 in that they have an occluding hydrophobic bridge across the active site that modulates substrate specificity.[36,37]

The diacidic biphenyl compounds (**2.1** – **2.3**) inhibit both OXA-24 and −58, although they are more potent inhibitors of OXA-58 (Table 4). Compound **2.2** is of particular interest in that it inhibits OXA-48 with a K_i of 4.3 μM and OXA-58 with a K_i of 1.8 μM. Although compound **2.2** exhibits a weaker, 70 μM K_i for OXA-24, it is the most potent diacidic biphenyl compound versus this enzyme. A comparison of the inhibition profiles of compounds **2.1** – **2.3** further indicates that the para-substituted diacid shows the broadest spectrum of inhibition towards the OXA carbapenemases examined (Table 4).

The naphthalene compounds (**3.1** – **3.5**) also inhibit OXA-24 and OXA-58, although with weaker potency than the biphenyl compounds (Table 4). Among these, compound **3.3** shows the broadest spectrum of inhibition, with K_i values of 12, 140, and 30 μM for OXA-48, −24, and −58, respectively. It is of interest that compound **3.3** is the most polar of the compounds tested, with amine and hydroxyl groups on the naphthalene rings in addition to the acids. Thus, polarity may be important for broad-spectrum inhibition. Note also that compound **3.1**, which is the most potent inhibitor of this class for OXA-48, is a weak inhibitor of OXA-24 and −58 ($K_i > 100$ μM), indicating the position of the diacid moieties is also important for the spectrum of inhibition.

The fluorene compounds (**4.1** – **4.3**) inhibit OXA-24 and −58 with a wide range in potencies (Table 4). However, as was observed with inhibition of OXA-48, the diacidic fluorene compound **4.3** is a much more potent inhibitor of OXA-24 and −58 than the monoacidic compounds **4.1** and **4.2**. Compound **4.3** is among the broadest spectrum inhibitors identified in this study, with K_i values of 1.4, 34, and 3.4 μM for OXA-48, −24, and −58, respectively. Coupled with the finding that compound **4.3** also permeates the *E. coli* outer membrane and potentiates ampicillin towards OXA-48 (Table 3), the results suggest this compound is a strong candidate for further medicinal chemistry optimization. In contrast, the monoacidic anthraquinone compounds **5.1** and **5.2** are weak inhibitors of all three OXA carbapenemases tested (Table 4).

Across the various scaffolds, OXA-24 was the least tractable of the enzymes for inhibition, with nearly all compounds showing reduced potency against OXA-24 in comparison to OXA-48 and OXA-58 (Table 4). The heterogeneity of class D enzymes makes it difficult to identify inhibitors with similar activity across enzymes.[7] For example, avibactam, a potent broad-spectrum β-lactamase inhibitor, shows reduced potency against OXA-24 compared to OXA-48.[38] However, from the compounds tested here, the azobenzene compound **6.1** inhibits all three carbapenemases with low micromolar potency (K_i values < 10 μM) and showed the best spectrum of activity. As noted above, it is unclear which configuration the azobenzene adopts for inhibition, since this scaffold can flip between *cis*- and *trans*-isomers upon exposure to UV light.[29] Nevertheless, due to more favorable thermodynamic stability, the *trans*-isomer is likely the dominant isomer in solution.[29] Note, however, that compound **6.1** showed the least synergy with ampicillin among the compounds tested for growth inhibition of *E. coli* expressing OXA-48, suggesting it may not accumulate across the outer membrane as efficiently as the other compounds (Table 3).

Developing inhibitors of class D carbapenemases is increasingly important due to the scarcity of potent inhibitors, particularly for OXA-48 given its prevalence in carbapenem-resistant *Enterobacteriaceae* across the globe.[4] The shift towards non-covalent inhibitors for OXA-48 and other class D enzymes is likely in part due to the unfavorable activity seen with many mechanism-based β-lactamase inhibitors.[7,38,39] The early inhibitors, clavulanic acid, sulbactam, and tazobactam, are β-lactam-based and more effective against class A β-lactamases than class D enzymes.[7] Additionally, many of the non-β-lactam inhibitors such as the bridged diazabicyclo[3.2.1]octanones (DBO) including avibactam are less effective against OXA-48 compared to the other serine β-lactamases.[38,40,41] This suggests the

development of non-covalent inhibitors might be a useful avenue to target more refractory enzymes that are not as susceptible to current inhibitors.

Previous fragment-based drug discovery (FBDD) efforts with OXA-48 suggest this approach can aid the design of novel non-covalent inhibitors.[18,19] FBDD screens can sample a wide range of chemical space and identify 'target interaction potential' or ligand-interacting regions within the target to guide compound optimization.[27] This approach can help study the inhibition of various β-lactamase and help customize inhibitors for efficient inhibition given their minimal size and complexity compared to larger combinatorial compounds. Extensive FBDD could help cluster enzymes based on their susceptibility to different scaffolds to facilitate designing inhibitors with a higher likelihood of efficacy for specific groups of enzymes. Identifying useful scaffolds will expedite the design of inhibitors, as many iterations can be created and tested against different β-lactamases.

In this study, we used an FBDD approach to identify OXA-48 inhibitors. Fragments tend to display millimolar potency due to their small size and limited functional groups[42], so the potency of the compounds identified here is promising. While multiple compounds of various scaffolds had K_i values below 50 μM, compounds **2.1**, **2.2**, **2.3**, **3.1**, **3.3**, **4.3**, and **6.1** were among the most potent (K_i values < 10 μM). Most of these compounds also had promising activity against other class D carbapenemases and showed activity in a microbiology assay. Trends in the inhibition data corroborate the usefulness of diacidic biphenyl- and naphthalene-based compounds. Although diacidic fragments have been previously shown to bind OXA-48[19], we also show they can inhibit OXA-58 as well as OXA-24, albeit to a lesser extent, opening the door to investigate these compounds in the design of broader spectrum class D carbapenemase inhibitors. OXA-48 inhibition is typically the most studied to gauge inhibitor activity on class D enzymes[43]; however, explicitly extending these studies to other class D carbapenemases can facilitate the design of broader spectrum inhibitors. We were also able to identify trends that can be exploited in future inhibitor designs, such as the increase in potency seen with carboxylic to sulfonic acid substitutions and with polar additions to diacidic naphthalenes. Several biphenyl-based compounds with a meta-configuration have previously been tested against OXA-48[19], however, we demonstrate that a para-configuration may be more useful for broader-spectrum inhibitors with added efficacy against the OXA-24 and OXA-58 carbapenemases. In addition to the previously identified biphenyls and naphthalenes, we demonstrated the potential of new scaffolds that have not been previously studied as β-lactamase inhibitors (fluorenes, anthraquinones, and azobenzenes).

Co-crystal structures of OXA-48 with compounds **2.2**, **2.3**, **3.1**, **3.3**, and **4.3** provided useful insights into how fragments can interact with active site residues for low micromolar inhibition. Diacids can be used to engage residues of the carboxylate binding pocket and Arg214 via hydrogen/ionic bonds. Also, the scaffolds represented make various hydrophobic/pi-stacking interactions despite their small size, suggesting the hydrophobic active site of OXA-48 can be exploited for the design of more effective inhibitors. For OXA-24 and OXA-58 inhibition, additional structural data are needed to determine whether their hydrophobic bridges play a significant role in their low susceptibility to several of the fragments when compared to OXA-48, which generally was more susceptible to inhibition

than the 'bridged' enzymes. Although OXA-24 and OXA-58 share a higher sequence identity and each has a hydrophobic bridge, OXA-58 was more susceptible to inhibition. Apart from the azobenzene-based compound, several diacids (compounds **2.1**, **2.2**, and **4.3**) displayed higher potency against OXA-58 than OXA-24. While further studies are required to confirm this phenomenon, the previously proposed plasticity of the OXA-58 active site may contribute to this property, which is advantageous for inhibitor development.[37] There are no reports of significant shifts in the structure of the OXA-24 active site. Compound **6.1**, the azobenzene, was very informative as the only compound to similarly inhibit all three carbapenemases. Additional studies, particularly structural data, may help explain how azobenzenes can inhibit unique class D β-lactamases. However, compound **6.1** was among the least effective compounds in the MIC assays, potentially due to it being larger than typical fragments (MW > 300 g/mol). Compound **6.1** also showed relatively low ligand efficiency (LE = 0.30) compared to other compounds, suggesting there may be a number of atoms inconsequential to activity that could potentially be removed. Future structure-activity relationship studies may help reduce the molecule size to improve ligand efficiency and accumulation into bacteria.

Methods

Protein expression and purification of OXA-24, OXA-48, and OXA-58

Each of the OXA enzymes was separately cloned into a pET28a vector for protein expression of the mature proteins. The thrombin site after the N-terminal His-tag in pET28a was replaced with a Tobacco Etch Virus (TEV) protease cleavage site. The constructed plasmids were transformed into *E. coli* BL21 (DE3) cells and single colonies were inoculated into Terrific Broth supplemented with kanamycin and grown overnight (TB_{kan}). The overnight culture was diluted 1:100 and grown to $OD_{600} = 0.6 – 0.8$. Protein expression was induced with a final concentration of 0.5mM Isopropyl β-D-1-thiogalactopyranoside (IPTG), and the culture was grown at 25°C for 18 – 20 hours. After pelleting and freezing, the cells were placed on ice and resuspended in 50 mM HEPES pH 7.5, 0.05% octyl β-D-glucopyranoside, shaken for 15 min, and sonicated as needed. Cell lysates were centrifuged (10,000 × g), filtered (0.45 μm filter), and passed through TALON Metal Affinity Resin (Takara Bio, Kusatsu, Japan) in Econo-Pac Chromatography Columns (Bio-Rad Laboratories, Hercules, CA). The resin was pre-washed with 50mM HEPES pH 7.5, 15 mM Na_2SO_4, and 20 mM imidazole. Gravity-flow was used to drain the lysate from the column and the resin was washed again. For each of the OXA protein preparations, the protein was eluted in multiple fractions of 50 mM HEPES, pH 7.5, 15 mM Na_2SO_4 buffer with increasing imidazole concentrations (70 mM, 80 mM, 90 mM, 100 mM, and 120 mM imidazole). Fractions were evaluated on SDS-PAGE for correct protein size and purity and then concentrated using 10 kDa MWCO Amicon Ultra-15 Centrifugal Filter Units (MilliporeSigma, Burlington, MA). After concentration and buffer exchange using the centrifugal filters, TEV cleavage reactions were performed overnight at 4°C. After TEV cleavage, the samples were incubated with TALON Metal Affinity Resin in chromatography columns (as described above) to remove the His-tagged TEV. The flow-through containing the cleaved proteins was collected in fractions, evaluated on SDS-PAGE gels, and then concentrated.

Inhibition assays and ligand efficiency metrics

The inhibition activity for all the fragment compounds was assessed using inhibition assays with nitrocefin as the reporter. For each of the OXA enzymes, steady-state kinetics was performed to determine the K_m values for the nitrocefin reporter substrate. Inhibition experiments were performed at nitrocefin concentrations below the K_m values in 50 mM HEPES pH 7.5, 15 mM NaHCO$_3$, 0.02% Tween20. A constant concentration of nitrocefin (30 μM), and enzyme were used for all experiments. The enzymes OXA-24, OXA-48 and OXA-58 were used at a constant concentration of 0.2 nM, 0.2 nM, and 0.1 nM respectively. Compounds were tested at up to 250 – 4000 μM, depending on solubility. The rate of nitrocefin hydrolysis was monitored at various compound concentrations using a Tecan M200 Infinite Pro plate reader (Tecan, Männedorf, Switzerland) and reaction rates were proxied by fitting progress curves to a one-phase decay equation to determine the rate constant. The rate constants were then fit to the Morrison Tight Binding equation to determine the inhibition constant (K_i). Ligand efficiency (LE) was calculated using a previously reported equation: LE = 1.37(pKi)/(# non-Hydrogen atoms).[44,45].

Compound sourcing and validation

All compounds were purchased from commercial vendors. Details of the vendors are given in Supplemental Information. In addition, we performed NMR validation on all the compounds and this data is provided in Supplemental Information. All the compound stocks were created by dissolving in either milli-Q water or dimethylsulfoxide (DMSO), depending on the solubility. Stocks were also made at varying concentrations due to differences in solubility. The DMSO tolerance of OXAs –24, –48, and –58 was tested and no more than 5% DMSO was used in final reactions for all the reactions.

Crystallography set-up and data collection

Crystallization experiments were set up in hanging drops using vapor diffusion. Crystallization buffers were screened by setting up drops manually in 24-well plates or 96-well plates using an automated Mosquito robot. Commercially available collections of crystallization conditions from Qiagen (Venlo, Netherlands), and Hampton Research (Aliso Viejo, CA) were screened in a 96-well format. Conditions were optimized as needed by altering pH and buffer/precipitant concentrations. Hanging drops were set up with a 100nL:100nL ratio of protein to reservoir solution and 250 μM OXA-48 was used to grow all the crystals that produced OXA-48 co-crystal structures. The structure with compound **2.3** was achieved by co-crystallizing OXA-48 with 2.5mM of compound **2.3** with a 0.1 M TRIS pH 8.5, 30% (v/v) PEG 400 reservoir solution. The remaining structures were achieved by soaking apo OXA-48 crystals formed in a 0.1 M TRIS pH 8.5, 25 % (v/v) PEG 550 MME solution. For crystal soaking experiments, stock solutions of each ligand were made using 100% 2-methyl-2,4-pentanediol (MPD). For compounds **2.2**, **3.1**, and **4.3**, the ligand stock in MPD was diluted with the reservoir solution of the crystal to be soaked (40:60) before adding a single 1μL drop to the hanging drop containing the OXA-48 apo crystal(s). For these structures, the final ligand concentration added to the corresponding hanging drop for soaking was 2mM. For compound **3.3**, the ligand stock made in MPD was diluted with the corresponding reservoir solution of the crystal to

be soaked (16.7:83.3) for a final concentration of 16.7 mM, and then a 2μL drop was added for soaking. Crystals were picked using either cryoloops (Hampton Research, Aliso Viejo, CA) or microloops (Mitegen, Ithaca, NY), and directly frozen in liquid nitrogen and shipped to the Berkeley Center for Structural Biology for data collection in the context of the Collaborative Crystallography Program. The data for the OXA-48 structures with compounds **2.2**, **3.1**, and **4.3** was collected from beamline 8.2.2, while the data for the structures with compounds **2.3** and **3.3** was collected from beamline 8.2.1.

Crystallography data processing, refinement, and analysis

All the diffraction data were integrated and scaled using either the HKL2000 software or IMOSFLM from the Collaborative Computational Project No. 4 (CCP4) software suite.[46,47] Integrations performed on IMOSFLM were scaled using the CCP4i2 SCALA software. All molecular replacements (PHASER program) and initial refining (REFMAC program) were performed using the CCP4 or CCP4i2 software.[48,49] Molecular replacement was used to determine the OXA-48 structures with the OXA-48 apo structure (PDB: 3HBR) as a search model. Additional refinements needed after the REFMAC refinement were performed using the PHENIX software (phenix.refine program).[50] For the refinements with PHENIX, Translation-Libration-Screw (TLS) parameters were used as needed, and the TLS groupings were derived from the TLSMD server via the PHENIX software. The Crystallography Object-Oriented Toolkit (COOT) software was used to manually adjust the structures as needed.[51] Structures were analyzed using the UCSF Chimera and Ligplot+ software to assess ligand binding, difference maps, and interactions of the ligands with OXA-48 residues.[52,53]

Bacterial susceptibility testing

Select compounds were tested for their ability to decrease the minimum inhibitory concentration of ampicillin (AMP MIC) needed to inhibit growth of *E. coli* expressing OXA-48. OXA-48 was cloned into the pTP145 vector as a fusion with the TEM β-lactamase signal sequence, under the transcriptional control of the *ampR* promoter.[54,55] The pTP145-OXA-48 plasmid was separately transformed into *E. coli* GKCW101 cells by electroporation.[56] Fresh colonies were, inoculated, and grown for 18 hours shaking at 37 °C. The micro broth dilution method was used to test the AMP MICs in sterile 96-well plates. AMP was tested at up to 2048 μg/mL while inhibitors were tested at up to 256 μg/mL, with a range of two-fold dilutions for each. For each bacterial culture tested, the saturated overnight culture was diluted 1:10^4 into the final solution. The final volume of all the wells was 200 μL. Since some compounds were dissolved in DMSO, the DMSO tolerance of the transformed bacteria was tested for its effect on the AMP MIC. No significant effect was seen at up to 5% DMSO. AMP MICs were incubated for 18 hours at 37 °C while shaking at 190 −200 rpm. AMP MICs were determined based on the visible appearance of bacterial growth.

Supplementary Material

Refer to Web version on PubMed Central for supplementary material.

Acknowledgments

References

(1). Papp-Wallace KM; Endimiani A; Taracila MA; Bonomo RA Carbapenems: Past, Present, and Future. Antimicrob. Agents Chemother 2011, 55 (11), 4943–4960. 10.1128/aac.00296-11. [PubMed: 21859938]

(2). Bonomo RA; Burd EM; Conly J; Limbago BM; Poirel L; Segre JA; Westblade LF Carbapenemase-Producing Organisms: A Global Scourge. Clin. Infect. Dis 2017, 66 (8), 1290–1297. 10.1093/cid/cix893.

(3). Nordmann P; Poirel L Epidemiology and Diagnostics of Carbapenem Resistance in Gram-Negative Bacteria. Clin. Infect. Dis 2019, 69 (Supplement_7), S521–S528. 10.1093/cid/ciz824. [PubMed: 31724045]

(4). Lee C-R; Lee JH; Park KS; Kim YB; Jeong BC; Lee SH Global Dissemination of Carbapenemase-Producing Klebsiella Pneumoniae: Epidemiology, Genetic Context, Treatment Options, and Detection Methods. Front Microbiol 2016, 7, 895. 10.3389/fmicb.2016.00895. [PubMed: 27379038]

(5). Tehrani KHME; Martin NI β-Lactam/β-Lactamase Inhibitor Combinations: An Update. Medchemcomm 2018, 9 (9), 1439–1456. 10.1039/c8md00342d. [PubMed: 30288219]

(6). Ambler RP The Structure of β-Lactamases. Philosophical Transactions Royal Soc. Lond. B Biological Sci 1980, 289 (1036), 321–331. 10.1098/rstb.1980.0049.

(7). Poirel L; Naas T; Nordmann P Diversity, Epidemiology, and Genetics of Class D β-Lactamases▽. Antimicrob. Agents Chemother 2010, 54 (1), 24–38. 10.1128/aac.01512-08. [PubMed: 19721065]

(8). Leonard DA; Bonomo RA; Powers RA Class D β-Lactamases: A Reappraisal after Five Decades. Accounts Chem. Res 2013, 46 (11), 2407–2415. 10.1021/ar300327a.

(9). Li J; Cross JB; Vreven T; Meroueh SO; Mobashery S; Schlegel HB Lysine Carboxylation in Proteins: OXA-10 B-lactamase. Proteins Struct. Funct. Bioinform 2005, 61 (2), 246–257. 10.1002/prot.20596.

(10). Maveyraud L; Golemi D; Kotra LP; Tranier S; Vakulenko S; Mobashery S; Samama J-P Insights into Class D β-Lactamases Are Revealed by the Crystal Structure of the OXA10 Enzyme from Pseudomonas Aeruginosa. Structure 2000, 8 (12), 1289–1298. 10.1016/s0969-2126(00)00534-7. [PubMed: 11188693]

(11). Golemi D; Maveyraud L; Vakulenko S; Samama J-P; Mobashery S Critical Involvement of a Carbamylated Lysine in Catalytic Function of Class D β-Lactamases. Proc. Nat. Acad. Sci 2001, 98 (25), 14280–14285. 10.1073/pnas.241442898. [PubMed: 11724923]

(12). Buchman JS; Schneider KD; Lloyd AR; Pavlish SL; Leonard DA Site-Saturation Mutagenesis of Position V117 in OXA-1 β-Lactamase: Effect of Side Chain Polarity on Enzyme Carboxylation and Substrate Turnover. Biochemistry 2012, 51 (14), 3143–3150. 10.1021/bi201896k. [PubMed: 22429123]

(13). Curley K; Pratt RF The Oxyanion Hole in Serine β-Lactamase Catalysis: Interactions of Thiono Substrates with the Active Site. Bioorg. Chem 2000, 28 (6), 338–356. 10.1006/bioo.2000.1184. [PubMed: 11352471]

(14). Ghuysen J-M Serine β-Lactamases and Penicillin-Binding Proteins. Ann. Rev. Microbiol 1991.

(15). Taylor DM; Anglin J; Park S; Ucisik MN; Faver JC; Simmons N; Jin Z; Palaniappan M; Nyshadham P; Li F; Campbell J; Hu L; Sankaran B; Prasad BVV; Huang H; Matzuk MM; Palzkill T Identifying Oxacillinase-48 Carbapenemase Inhibitors Using DNA-Encoded Chemical Libraries. ACS Infect. Dis 2020, 6 (5), 1214–1227. 10.1021/acsinfecdis.0c00015. [PubMed: 32182432]

(16). Warr WA Fragment-Based Drug Discovery. J. Comput. Aid. Mol. Des 2009, 23 (8), 453–458. 10.1007/s10822-009-9292-1.

(17). Edfeldt FNB; Folmer RHA; Breeze AL Fragment Screening to Predict Druggability (Ligandability) and Lead Discovery Success. Drug Discov. Today 2011, 16 (7–8), 284–287. 10.1016/j.drudis.2011.02.002. [PubMed: 21315179]

(18). Lund BA; Christopeit T; Guttormsen Y; Bayer A; Leiros H-KS Screening and Design of Inhibitor Scaffolds for the Antibiotic Resistance Oxacillinase-48 (OXA-48) through Surface Plasmon Resonance Screening. J. Med. Chem 2016, 59 (11), 5542–5554. 10.1021/acs.jmedchem.6b00660. [PubMed: 27165692]

(19). Akhter S; Lund BA; Ismael A; Langer M; Isaksson J; Christopeit T; Leiros H-KS; Bayer A A Focused Fragment Library Targeting the Antibiotic Resistance Enzyme - Oxacillinase-48: Synthesis, Structural Evaluation and Inhibitor Design. Eur. J. Med. Chem 2018, 145, 634–648. 10.1016/j.ejmech.2017.12.085. [PubMed: 29348071]

(20). Eidam O; Romagnoli C; Dalmasso G; Barelier S; Caselli E; Bonnet R; Shoichet BK; Prati F Fragment-Guided Design of Subnanomolar β-Lactamase Inhibitors Active in Vivo. Proc. Nat. Acad. Sci 2012, 109 (43), 17448–17453. 10.1073/pnas.1208337109. [PubMed: 23043117]

(21). Nichols DA; Renslo AR; Chen Y Fragment-Based Inhibitor Discovery against β-Lactamase. Future Med. Chem 2014, 6 (4), 413–427. 10.4155/fmc.14.10. [PubMed: 24635522]

(22). Ramadan RA; Gebriel MG; Kadry HM; Mosallem A Carbapenem-Resistant Acinetobacter Baumannii and Pseudomonas Aeruginosa: Characterization of Carbapenemase Genes and E-Test Evaluation of Colistin-Based Combinations. Infect. Drug Resist 2018, 11, 1261–1269. 10.2147/idr.s170233. [PubMed: 30197524]

(23). Hussein EM; Alsantali RI; Morad M; Obaid RJ; Altass HM; Sayqal A; Abourehab MAS; Elkhawaga AA; Aboraia ASM; Ahmed SA Bioactive Fluorenes. Part III: 2,7-Dichloro-9H-Fluorene-Based Thiazolidinone and Azetidinone Analogues as Anticancer and Antimicrobial against Multidrug Resistant Strains Agents. BMC Chem 2020, 14 (1), 42. 10.1186/s13065-020-00694-2. [PubMed: 32596690]

(24). Sessa L; Concilio S; Iannelli P; Santis FD; Porta A; Piotto S Antimicrobial Azobenzene Compounds and Their Potential Use in Biomaterials. Aip Conf. Proc 2016, 1727 (1), 020018. 10.1063/1.4945973.

(25). Monaghan C; Holland S; Dale JW The Interaction of Anthraquinone Dyes with the Plasmid-Mediated OXA-2 β-Lactamase. Biochem. J 1982, 205 (2), 413–417. 10.1042/bj2050413. [PubMed: 6982708]

(26). Congreve M; Carr R; Murray C; Jhoti HA 'Rule of Three' for Fragment-Based Lead Discovery? Drug Discov. Today 2003, 8 (19), 876–877. 10.1016/s1359-6446(03)02831-9.

(27). Kenny PW The Nature of Ligand Efficiency. J. Cheminformatics 2019, 11 (1), 8. 10.1186/s13321-019-0330-2.

(28). Zhu T; Cao S; Su P-C; Patel R; Shah D; Chokshi HB; Szukala R; Johnson ME; Hevener KE Hit Identification and Optimization in Virtual Screening: Practical Recommendations Based on a Critical Literature Analysis. J. Med. Chem 2013, 56 (17), 6560–6572. 10.1021/jm301916b. [PubMed: 23688234]

(29). Samanta D; Gemen J; Chu Z; Diskin-Posner Y; Shimon LJW; Klajn R Reversible Photoswitching of Encapsulated Azobenzenes in Water. Proc. Nat. Acad. Sci 2018, 115 (38), 9379–9384. 10.1073/pnas.1712787115. [PubMed: 29717041]

(30). Cabré G; Garrido-Charles A; Moreno M; Bosch M; Porta-de-la-Riva M; Krieg M; Gascón-Moya M; Camarero N; Gelabert R; Lluch JM; Busqué F; Hernando J; Gorostiza P; Alibés R Rationally Designed Azobenzene Photoswitches for Efficient Two-Photon Neuronal Excitation. Nat. Commun 2019, 10 (1), 907. 10.1038/s41467-019-08796-9. [PubMed: 30796228]

(31). Docquier J-D; Calderone V; Luca FD; Benvenuti M; Giuliani F; Bellucci L; Tafi A; Nordmann P; Botta M; Rossolini GM; Mangani S Crystal Structure of the OXA-48 β-Lactamase Reveals Mechanistic Diversity among Class D Carbapenemases. Chem. Biol 2009, 16 (5), 540–547. 10.1016/j.chembiol.2009.04.010. [PubMed: 19477418]

(32). CLSI. M100: Performance Standards for Antimicrobial Susceptibility 30th Ed. Clinical and Laboratory Standards Institute 2018.

(33). Zgurskaya HI; López CA; Gnanakaran S Permeability Barrier of Gram-Negative Cell Envelopes and Approaches To Bypass It. ACS Infect. Dis 2015, 1 (11), 512–522. 10.1021/ acsinfecdis.5b00097. [PubMed: 26925460]

(34). Poirel L; Nordmann P Carbapenem Resistance in Acinetobacter Baumannii: Mechanisms and Epidemiology. Clin. Microbiol. Infec 2006, 12 (9), 826–836. 10.1111/j.1469-0691.2006.01456.x. [PubMed: 16882287]

(35). Pogue JM; Mann T; Barber KE; Kaye KS Carbapenem-Resistant Acinetobacter Baumannii: Epidemiology, Surveillance and Management. Expert Rev. Anti-Infect 2014, 11 (4), 383–393. 10.1586/eri.13.14.

(36). Docquier J-D; Mangani S Structure-Function Relationships of Class D Carbapenemases. Curr. Drug Targets 2016, 17 (9), 1061–1071. 10.2174/1389450116666150825115824. [PubMed: 26302798]

(37). Saino H; Sugiyabu T; Ueno G; Yamamoto M; Ishii Y; Miyano M Crystal Structure of OXA-58 with the Substrate-Binding Cleft in a Closed State: Insights into the Mobility and Stability of the OXA-58 Structure. PLOS One 2015, 10 (12), e0145869. 10.1371/journal.pone.0145869. [PubMed: 26701320]

(38). Ehmann DE; Jahi H; Ross PL; Gu R-F; Hu J; Durand-Réville TF; Lahiri S; Thresher J; Livchak S; Gao N; Palmer T; Walkup GK; Fisher SL Kinetics of Avibactam Inhibition against Class A, C, and D β-Lactamases. J. Biol. Chem 2013, 288 (39), 27960–27971. 10.1074/jbc.m113.485979. [PubMed: 23913691]

(39). Drawz SM; Bonomo RA Three Decades of β-Lactamase Inhibitors. Clin. Microbiol. Rev 2010, 23 (1), 160–201. 10.1128/cmr.00037-09. [PubMed: 20065329]

(40). Bush K; Bradford PA Interplay between β-Lactamases and New β-Lactamase Inhibitors. Nat. Rev. Microbiol 2019, 17 (5), 295–306. 10.1038/s41579-019-0159-8. [PubMed: 30837684]

(41). Lahiri SD; Mangani S; Jahi H; Benvenuti M; Durand-Reville TF; Luca FD; Ehmann DE; Rossolini GM; Alm RA; Docquier J-D Molecular Basis of Selective Inhibition and Slow Reversibility of Avibactam against Class D Carbapenemases: A Structure-Guided Study of OXA-24 and OXA-48. ACS Chem. Biol 2015, 10 (2), 591–600. 10.1021/cb500703p. [PubMed: 25406838]

(42). Lamoree B; Hubbard RE Current Perspectives in Fragment-Based Lead Discovery (FBLD). Essays Biochem 2017, 61 (5), 453–464. 10.1042/ebc20170028. [PubMed: 29118093]

(43). Vázquez-Ucha JC; Arca-Suárez J; Bou G; Beceiro A New Carbapenemase Inhibitors: Clearing the Way for the β-Lactams. Int. J. Mol. Sci 2020, 21 (23), 9308. 10.3390/ijms21239308.

(44). Hopkins AL; Keserü GM; Leeson PD; Rees DC; Reynolds CH The Role of Ligand Efficiency Metrics in Drug Discovery. Nat. Rev. Drug Discov 2014, 13 (2), 105–121. 10.1038/nrd4163. [PubMed: 24481311]

(45). Verdonk ML; Rees DC Group Efficiency: A Guideline for Hits-to-Leads Chemistry. ChemMedChem 2008, 3 (8), 1179–1180. 10.1002/cmdc.200800132. [PubMed: 18651625]

(46). Otwinowski Z; Minor W 20: Processing of X-Ray Diffraction Data Collected in Oscillation Mode; Methods in Enzymology; Academic Press, 1997; Vol. 276.

(47). Battye TGG; Kontogiannis L; Johnson O; Powell HR; Leslie AGW IMOSFLM: A New Graphical Interface for Diffraction-Image Processing with MOSFLM. Acta Crystallogr. Sect. D Biological Crystallogr 2011, 67 (Pt 4), 271–281. 10.1107/s0907444910048675.

(48). McCoy AJ; Grosse-Kunstleve RW; Adams PD; Winn MD; Storoni LC; Read RJ Phaser Crystallographic Software. J. Appl. Crystallogr 2007, 40 (4), 658–674. 10.1107/ s0021889807021206. [PubMed: 19461840]

(49). Murshudov GN; Skubák P; Lebedev AA; Pannu NS; Steiner RA; Nicholls RA; Winn MD; Long F; Vagin AA REFMAC5 for the Refinement of Macromolecular Crystal Structures. Acta Crystallogr. Sect D Biological Crystallogr 2011, 67 (4), 355–367. 10.1107/s0907444911001314.

(50). Adams PD; Afonine PV; Bunkóczi G; Chen VB; Davis IW; Echols N; Headd JJ; Hung L-W; Kapral GJ; Grosse-Kunstleve RW; McCoy AJ; Moriarty NW; Oeffner R; Read RJ; Richardson DC; Richardson JS; Terwilliger TC; Zwart PH PHENIX: A Comprehensive Python-Based System for Macromolecular Structure Solution. Acta Crystallogr. Sect. D Biolog. Crystallogr 2010, 66 (Pt 2), 213–221. 10.1107/s0907444909052925.

(51). Emsley P; Cowtan K Coot: Model-Building Tools for Molecular Graphics. Acta Crystallogr. Sect. D Biological Crystallogr 2004, 60 (12), 2126–2132. 10.1107/s0907444904019158.

(52). Pettersen EF; Goddard TD; Huang CC; Couch GS; Greenblatt DM; Meng EC; Ferrin TE UCSF Chimera—A Visualization System for Exploratory Research and Analysis. J. Comput. Chem 2004, 25 (13), 1605–1612. 10.1002/jcc.20084. [PubMed: 15264254]

(53). Laskowski RA; Swindells MB LigPlot+: Multiple Ligand–Protein Interaction Diagrams for Drug Discovery. J. Chem. Inf. Model 2011, 51 (10), 2778–2786. 10.1021/ci200227u. [PubMed: 21919503]

(54). Kong K-F; Jayawardena SR; Indulkar SD; Puerto A del; Koh, C.-L.; Høiby, N.; Mathee, K. Pseudomonas Aeruginosa AmpR Is a Global Transcriptional Factor That Regulates Expression of AmpC and PoxB β-Lactamases, Proteases, Quorum Sensing, and Other Virulence Factors. Antimicrob. Agents Chemother 2005, 49 (11), 4567–4575. 10.1128/aac.49.11.4567-4575.2005. [PubMed: 16251297]

(55). Huang W; McKevitt M; Palzkill T Use of the Arabinose Pbad Promoter for Tightly Regulated Display of Proteins on Bacteriophage. Gene 2000, 251 (2), 187–197. 10.1016/s0378-1119(00)00210-9. [PubMed: 10876095]

(56). Krishnamoorthy G; Wolloscheck D; Weeks JW; Croft C; Rybenkov VV; Zgurskaya HI Breaking the Permeability Barrier of *Escherichia coli* by Controlled Hyperporination of the Outer Membrane. Antimicrob. Agents Chemother 2016, 60 (12), 7372–7381. 10.1128/aac.01882-16. [PubMed: 27697764]
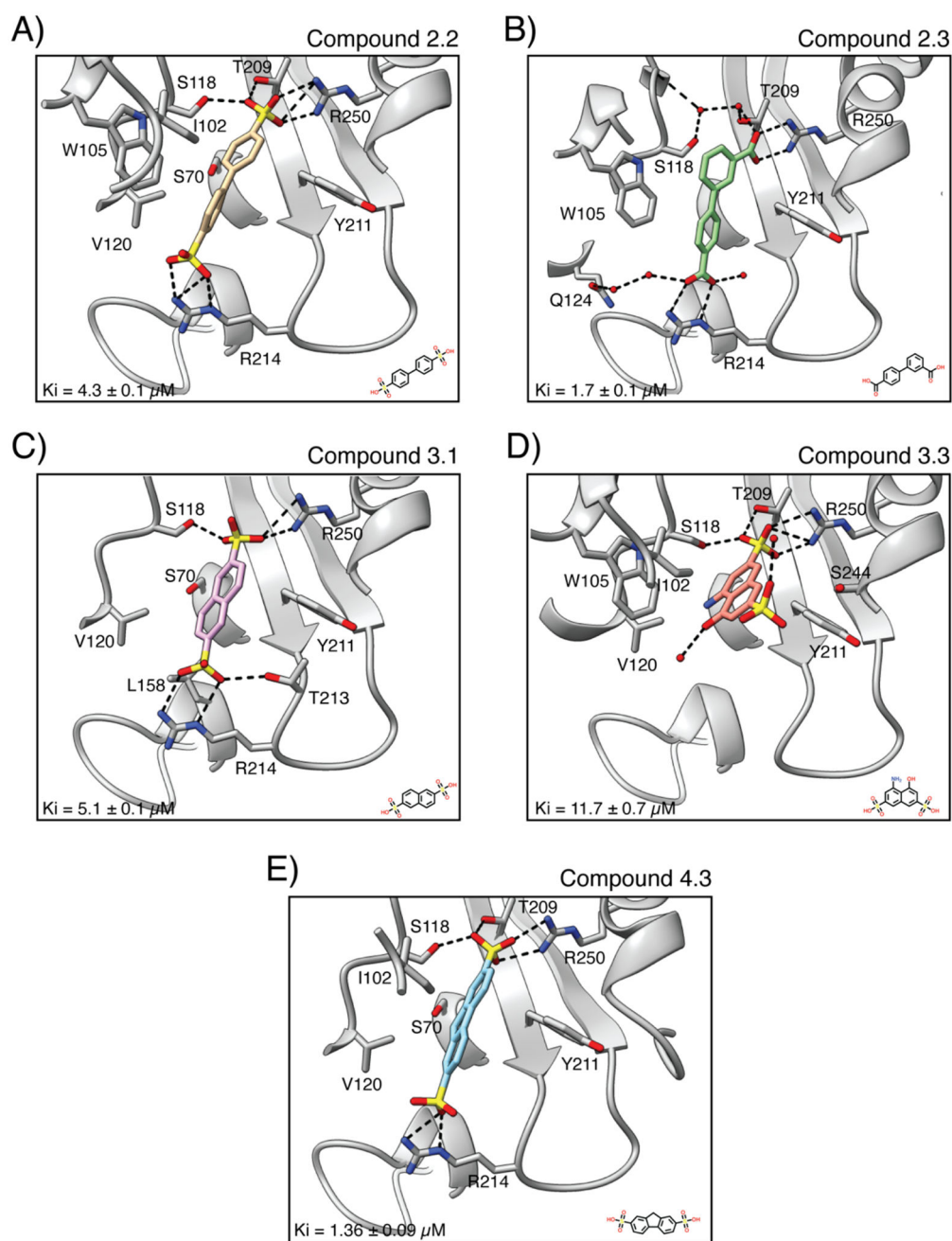
Figure 1.
Low micromolar fragment inhibitors form various hydrogen bonds and hydrophobic interactions, and additional residues that participate in either a hydrophobic/van der Waals interaction or pi-stacking interaction with the corresponding inhibitor are shown. **A**. Compound 2.2 (tan) in complex with OXA-48 β-lactamase (gray ribbon). Oxygen is shown in red, nitrogen in blue, and sulfur in yellow. The K_i for inhibition of OXA-48 is indicated at the bottom left of the panel. The chemical structure of the compound is shown at the bottom right of the panel. OXA-48 residues are labeled. **B**. Compound 2.3 (green)/OXA-48.

C. Compound 3.1 (pink)/OXA-48. **D**. Compound 3.3 (salmon)/OXA-48. **E**. Compound 4.3 (cyan)/OXA-48.

Table 1.

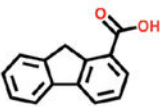Potency and ligand efficiency of compounds towards OXA-48 β-lactamase.
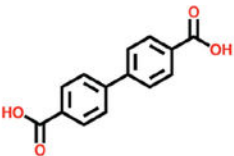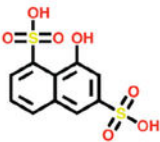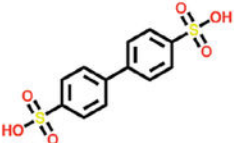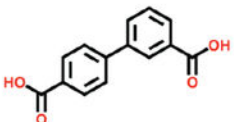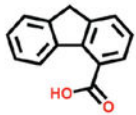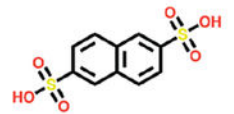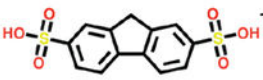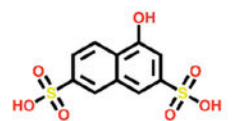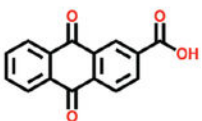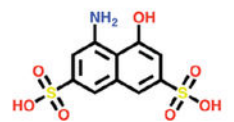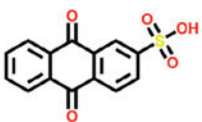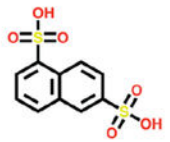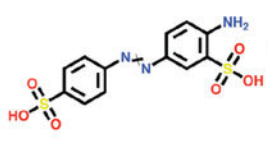
I.D.	Compound	Ki (μM) (LE)	I.D.	Compound	Ki (μM) (LE)
2.1		15 ± 1 (0.37)	3.5		96.7 ± 0.8 (0.29)
2.2		4.3 ± 0.1 (0.41)	4.1		257 ± 8 (0.31)
2.3		1.7 ± 0.1 (0.44)	4.2		409 ± 27 (0.29)
3.1		5.1 ± 0.1 (0.40)	4.3		1.36 ± 0.09 (0.38)
3.2		50.0 ± 0.5 (0.29)	5.1		52 ± 2 (0.31)
3.3		11.7 ± 0.7 (0.34)	5.2		76 ± 3 (0.28)
3.4		267 ± 19 (0.27)	6.1		7.9 ± 0.4 (0.30)

Table 2.

Crystallography statistics for structures of OXA-48 in complex with compounds **2.2**, **2.3**, **3.1**, **3.3**, **4.3**.

	Cmpd 2.2: OXA-48 (PDB: 6XQR)	Cmpd 2.3: OXA-48 (PDB: 7JHQ)	Cmpd 3.1: OXA-48 (PDB: 7K5V)	Cmpd 3.3: OXA-48 (PDB: 7R6Z)	Cmpd 4.3: OXA-48 (PDB: 7L8O)
Resolution range	29.44 – 2.201 (2.28 – 2.201)	34.84 – 2.0 (2.071 – 2.0)	29.61 – 2.801 (2.901 – 2.801)	34.35 – 2.1 (2.175 – 2.1)	48.6 – 2.702 (2.798 – 2.702)
Space group	P 65 2 2	P 65	P 65 2 2	P 65 2 2	P 65
Unit Cell (a, b, c) (Å)	122.561, 122.561, 161.284	120.68, 120.68, 159.769	122.922, 122.922, 161.143	121.808, 121.808, 160.462,	122.039, 122.039, 160.787
Unit Cell (α, β, γ) (°)	90, 90, 120	90, 90, 120	90, 90, 120	90, 90, 120	90, 90, 120
Unique reflections	36847 (3626)	88743 (8880)	18259 (1751)	41571 (4062)	37105 (3638)
Completeness (%)	99.91 (100.00)	99.90 (99.81)	99.65 (97.88)	99.92 (100.00)	99.68 (98.03)
Mean I/sigma(I)	30.1	9.3	24.4	34.125	19.3
Wilson B-factor	29.76	30.58	47.53	23.94	40.34
R-merge	0.121	0.122	0.138	0.137	0.134
R-meas	0.125	0.128	0.143	0.14	0.14
R-pim	0.028	0.037	0.035	0.027	0.042
CC1/2	0.963	0.998	0.961	0.959	0.941
Reflections used in refinement	36841 (3626)	88675 (8864)	18257 (1751)	41554 (4062)	37067 (3638)
Reflections used for R-free	1866 (180)	4385 (435)	960 (96)	2038 (181)	1865 (156)
R-work	0.1681 (0.2296)	0.1696 (0.2726)	0.1925 (0.2685)	0.1663 (0.1814)	0.1684 (0.2149)
R-free	0.2030 (0.2976)	0.2127 (0.3055)	0.2369 (0.3117)	0.1956 (0.2437)	0.2106 (0.2809)
Overall MolProbity score	0.96	1.2	1.18	1.02	1.28
Number of non-hydrogen atoms	4300	8607	4009	4329	8109
macromolecules	3964	7880	3964	3964	7916
ligands	41	108	45	66	121
solvent	295	619	N/A	299	72
Protein residues	484	968	484	484	979
RMS(bonds)	0.003	0.003	0.003	0.002	0.006
RMS(angles)	0.59	0.56	0.6	0.48	0.75
Ramachandran favored (%)	97.68	97.05	97.26	97.68	96.31
Ramachandran allowed (%)	2.32	2.74	2.74	2.32	3.69
Ramachandran outliers (%)	0	0.21	0	0	0
Rotamer outliers (%)	0	0	0	0.24	0
Clashscore	1.52	2.48	2.41	1.89	2.47
Average B-factor	37	39.36	44.75	30.88	45.35
macromolecules	36.67	38.83	44.52	30.13	45.15
ligands	39.01	43.24	64.45	48.25	65.94
solvent	41.2	45.37	N/A	37.02	32.71

	Cmpd 2.2: OXA-48 (PDB: 6XQR)	Cmpd 2.3: OXA-48 (PDB: 7JHQ)	Cmpd 3.1: OXA-48 (PDB: 7K5V)	Cmpd 3.3: OXA-48 (PDB: 7R6Z)	Cmpd 4.3: OXA-48 (PDB: 7L8O)
Number of TLS groups	12	27	13	15	21

Table 3.

Synergy of compounds with ampicillin versus *E. coli* expressing OXA-48 (*E. coli*_{OXA-48}).

Cmpd (µg/ml)	Ampicillin MICs for *E. coli*$_{OXA-48}$ (µg/ml)						
	2.1	2.2	2.3	3.1	3.3	4.3	6.1
0	512	512	1024	512	512	512	512
4	512	512	512	256	512	256	512
8	512	512	512	256	512	256	512
16	512	512	512	256	512	256	512
32	512	256	256	128	512	256	256
64	256	128	256	128	512	128	256
128	256	64	128	64	256	64	256
256	128	32	64	32	128	32	128
[a]K_i (µg/ml)	3.6	1.4	0.4	1.7	4.1	0.5	3.0

[a]The K_i value for inhibition of OXA-48 for each compound expressed as µg/ml.

Table 4.

Inhibition potency and ligand efficiency of compounds towards the OXA-48, OXA-24 and OXA-58 carbapenemases.

compound	OXA-48		OXA-24		OXA-58	
	K_i (μM)	LE[a]	K_i (μM)	LE	K_i (μM)	LE
2.1	15 ± 1	0.37	87 ± 3	0.31	12.9 ± 0.1	0.37
2.2	4.3 ± 0.1	0.41	70 ± 3	0.32	1.8 ± 0.1	0.44
2.3	1.7 ± 0.1	0.44	118.4 ± 0.9	0.30	45.8 ± 0.6	0.33
3.1	5.1 ± 0.1	0.40	150 ± 6	0.29	120 ± 5	0.30
3.2	50.0 ± 0.5	0.29	520 ± 33	0.22	410 ± 1	0.23
3.3	11.7 ± 0.8	0.34	140 ± 7	0.26	30 ± 2	0.31
3.4	267 ± 19	0.27	3200 ± 18	0.19	2100 ± 260	0.20
3.5	96.7 ± 0.8	0.29	330 ± 19	0.25	500 ± 21	0.24
4.1	257 ± 8	0.31	2300 ± 250	0.23	270 ± 4	0.31
4.2	410 ± 27	0.29	>2000	N/A[b]	2100 ± 170	0.23
4.3	1.36 ± 0.09	0.38	34 ± 1	0.29	3.4 ± 0.3	0.36
5.1	52 ± 2	0.31	480 ± 19	0.24	120 ± 13	0.28
5.2	76 ± 3	0.28	920 ± 23	0.21	93 ± 2	0.28
6.1	7.9 ± 0.4	0.30	7.9 ± 0.6	0.30	1.7 ± 0.1	0.34

[a]Ligand efficiency. Calculated as described in Methods.

[b]N/A - not applicable